

SUPPLEMENTAL MATERIAL

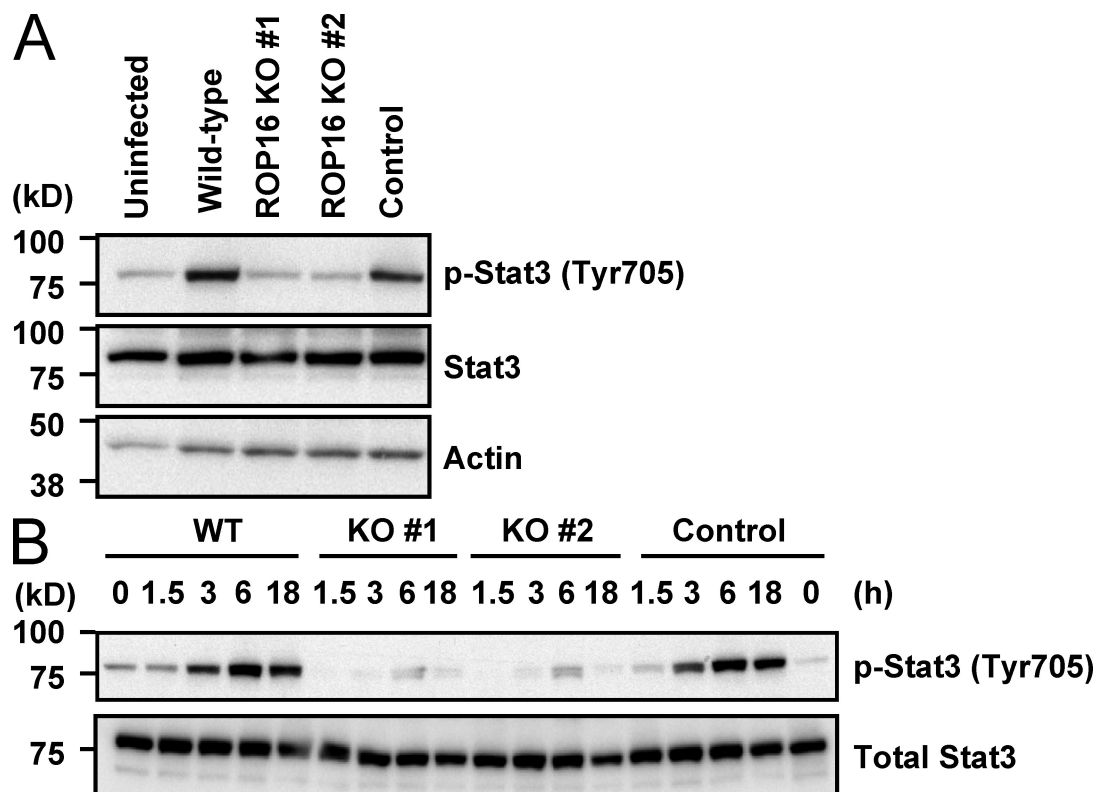
Yamamoto et al., <http://www.jem.org/cgi/content/full/jem.20091703/DC1>

Figure S1. Defective time-dependent Stat3 activation in cells infected with ROP16-deficient parasites. Serum-starved MEFs were infected with an MOI = 10 of the indicated parasites for 18 h (A) or the indicated time periods (B). Activation of Stat3 was also determined by Western blotting on cell extracts using anti-phospho-Stat3 Tyr 705. Stat3 levels are shown as loading controls. Data are representative of at least three independent experiments.

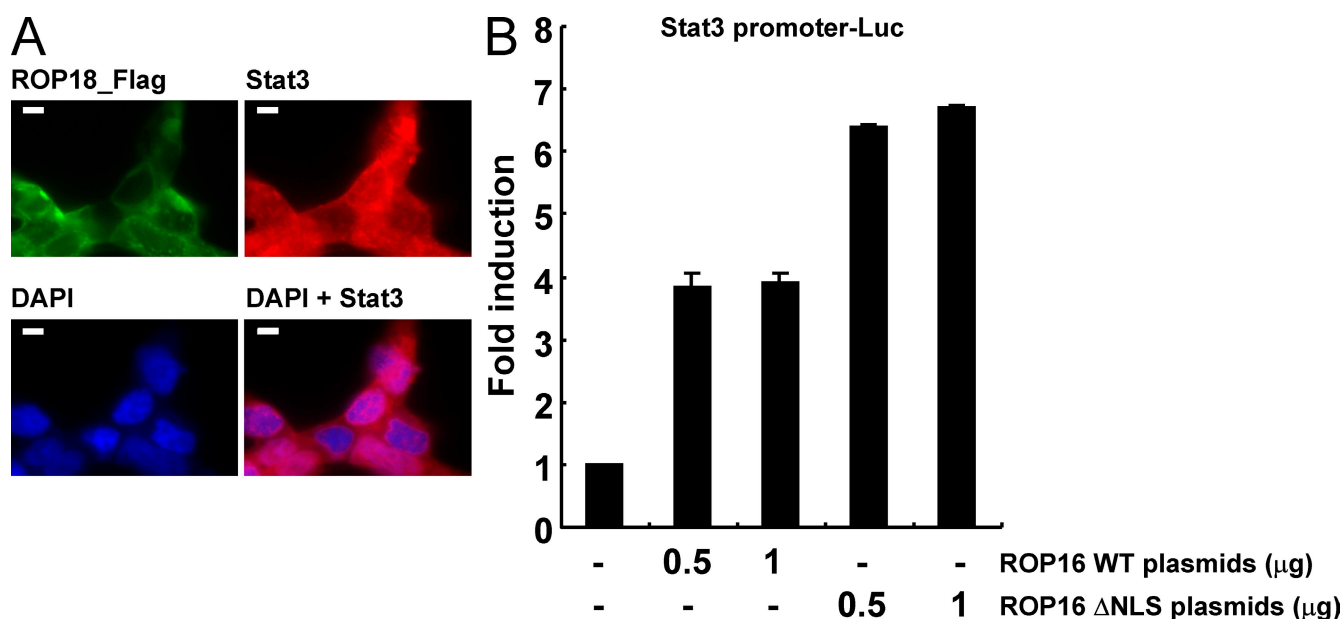


Figure S2. Cytoplasmic Stat3 localization in ROP18-transfected cells and activation of the Stat3-dependent promoter in cells transfected with NLS-mutated ROP16. (A) 293T cells were transfected with Flag-tagged ROP18 expression vectors. 48 h after transfection, the cells were fixed and stained with anti-STAT3 or anti-Flag and revealed with Alexa Fluor 488-conjugated anti-mouse IgG (green), Alexa Fluor 594-conjugated anti-rabbit IgG antibody (red), or DAPI (blue). Bars, 10 μ m. (B) 293T cells were transfected with the indicated Stat3-dependent luciferase reporters together with the indicated expression vectors. Luciferase activities were expressed as fold increases over the background levels shown by lysates prepared from mock-transfected cells. Indicated values are means \pm the variation range of duplicates. Data are representative of two independent experiments.

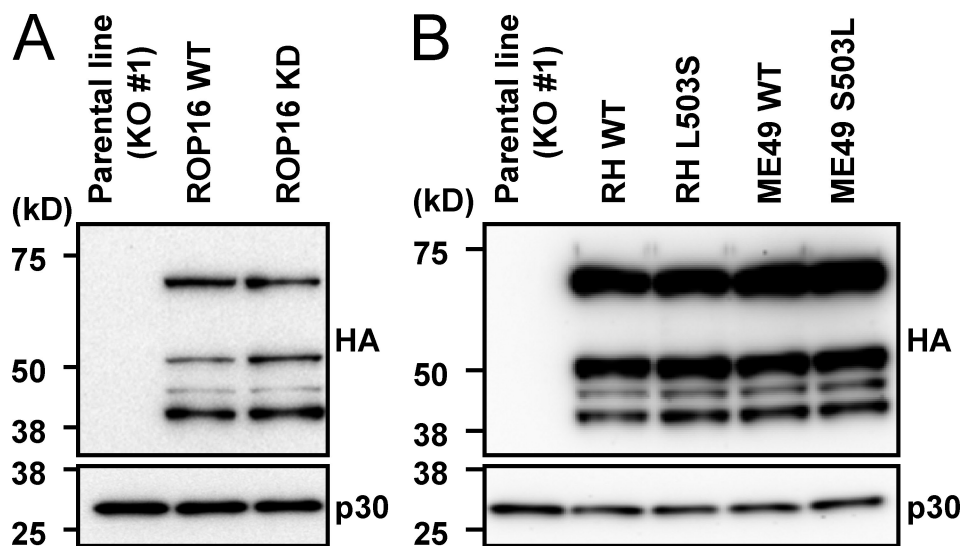


Figure S3. Complementation of ROP16-deficient parasites by ROP16 mutants. ROP16-deficient parental parasites were transfected with the indicated expression vectors. After pyrimethamine selection and cloning by limiting dilution, the parasites were lysed and subjected to Western blot. Expression of each ROP16 mutant was also determined by Western blot analysis of total cell lysates extracts using anti-HA antibodies. Expression levels of p30 antigens were analyzed and shown as loading controls. Data are representative of two independent experiments.

RH	373	PIALYNRGHLGSGHFGAVIKASLDDGTLYAAKVPYSQIVPNADAT	417

ME49	373	PIALYNRGHLGSGHFGAVIKASLDDGTLYAAKVPYSQIVPNADAT	417
RH	418	SAELEAGISSARAELVKTIRQELDVRDKLVAKGLTLTETVSQYGL	462
		*****_*****_****	
ME49	418	SAELEAEISSARAELVKTIRQELDVRDKLVAKGLTLTETAEQYGL	462
RH	463	PLCQMTLTLPENKATVVRSGSRLFVVSKEVMLLPLIDGSALNSLV	507
		*****_****	
ME49	463	PLCQMTLTLPENKATVVRSGSRLVVVSKEVMLLPLIDGSPSNLSLV	507
RH	508	QSQPPFLFQRAVAREAILALAKLHELGFAGHDVKLNMMI	547
		*****_*****	
ME49	508	QSQPPFLFQRAVAREAIIALAKLHELGFAGHDVKLNMMI	547

Figure S4. Amino acid sequences of type I and type II ROP16 at position 373–547. The predicted amino acid sequence for the primary translation product of the *ROP16* gene is shown for type I parasites (top line). The sequences for type II parasites are shown on the second line with a dash to indicate identity to the type I sequence.

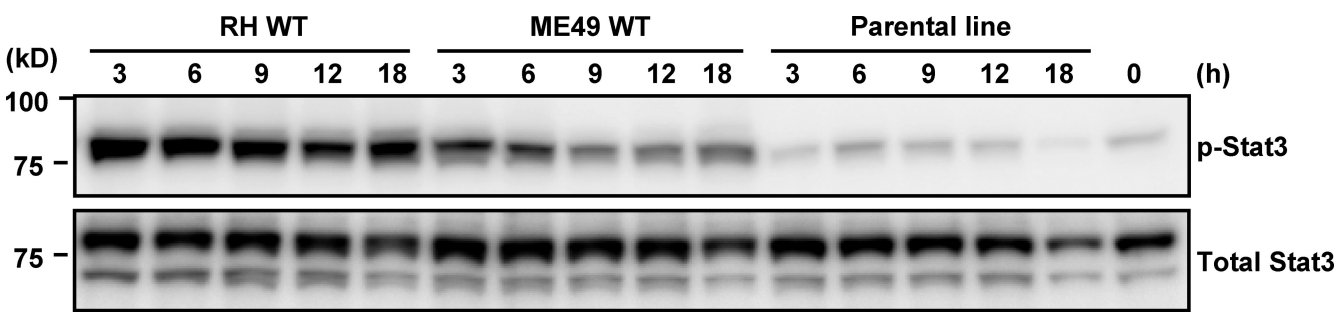


Figure S5. Time-dependent Stat3 activation in cells infected with ROP16–complemented parasites. Serum-starved MEFs were infected with an MOI = 10 of the indicated parasites for the indicated time periods. Activation of Stat3 was also determined by Western blot analysis of cell extracts using anti-phospho-Stat3 Tyr 705. Stat3 levels are shown as loading controls. Data are representative of three independent experiments.

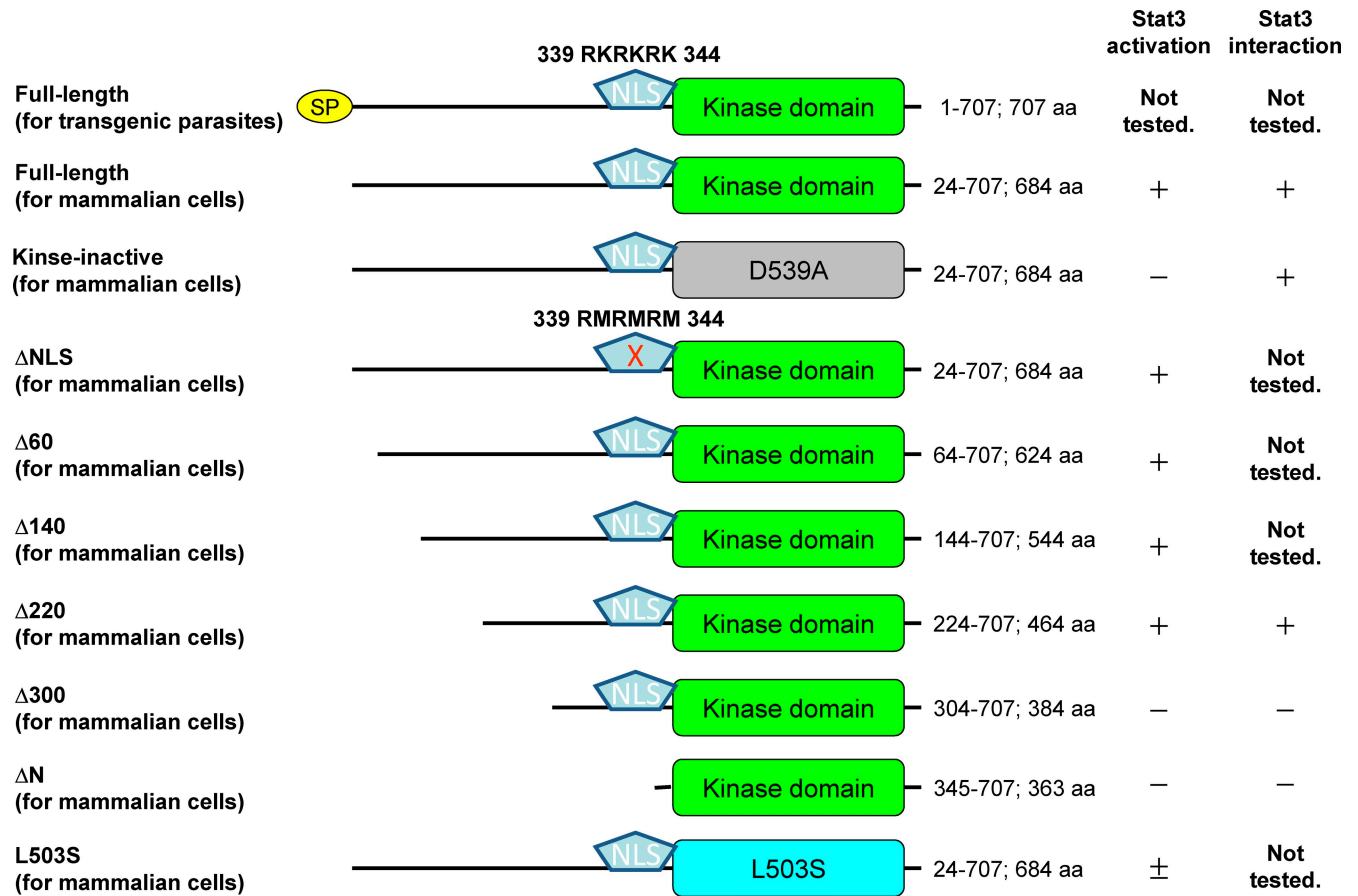


Figure S6. Type I ROP16 deletion and point mutants. SP, signal peptide. Whether the indicated ROP16 activates or interacts with Stat3 in 293T cells are shown in the right two columns.

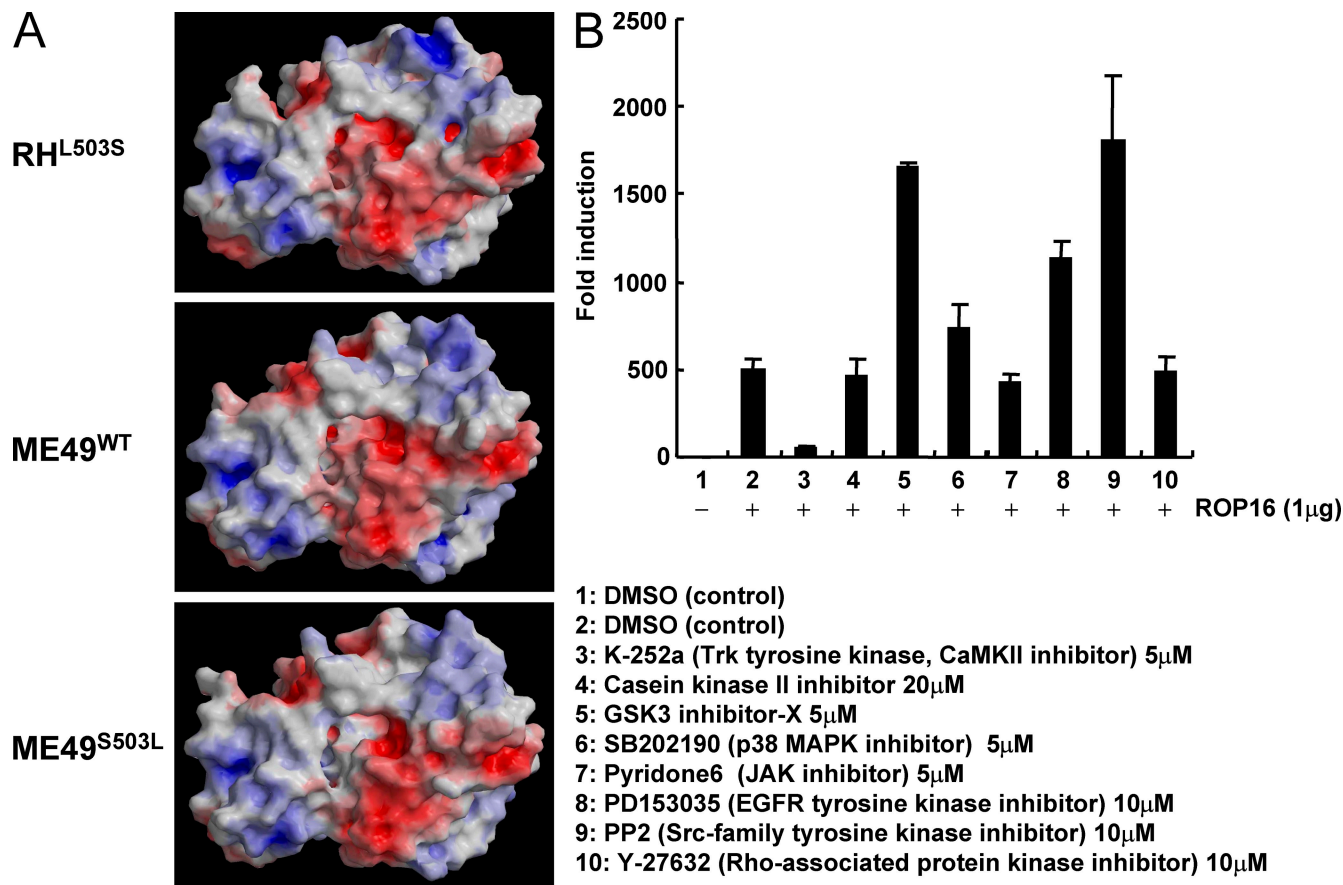


Figure S7. In silico modeling of ROP16 variants and screening of kinase inhibitors. (A) Molecular surfaces of RH^{L503S}, ME49^{WT}, and ME49^{S503L} are shown. Model calculations and figure preparation methods were identical those of RH^{WT} model. (B) 293T cells were transfected with the APRF-luc reporters together with 1 μg of empty or Flag-tagged ROP16 (ROP16WT) expression vectors in the presence of the indicated kinase inhibitors with the indicated concentrations or DMSO (control). Luciferase activities were expressed as fold increases over the background levels shown by lysates prepared from mock-transfected cells. Indicated values are means ± the variation range of duplicates. Data are representative of two independent calculations (A) or two independent experiments (B).

Table S1. The 20 most similar kinases to the RH^{WT} model, according to SeSAW, using the Spanner model built from SCOP domain d1s9jA

PDB ID	Kinase name	Score	ID
			%
3dy7A	Dual specificity mitogen-activated protein kinase kinase 1	334.5	20
3eqfA	Dual specificity mitogen-activated protein kinase kinase 1	326.8	18
3eqiA	Dual specificity mitogen-activated protein kinase kinase 1	323.7	18
1s9iB	Dual specificity mitogen-activated protein kinase kinase 2	323.0	20
2r5tA	Serine/threonine-protein kinase Sgk1	315.6	22
2iwiA	Serine/threonine-protein kinase Pim-2	315.0	20
3eqcA	Dual specificity mitogen-activated protein kinase kinase 1	314.2	18
1urcA	Cell division protein kinase 2	312.3	20
2j0iA	Serine/threonine-protein kinase PAK 4	312.2	19
1s9jA	Dual specificity mitogen-activated protein kinase kinase 1	311.9	18
2cdzA	Serine/threonine-protein kinase PAK 4	310.1	20
1zrzA	Protein kinase C iota type	309.1	20
3eqdA	Dual specificity mitogen-activated protein kinase kinase 1	307.0	18
2p55A	Dual specificity mitogen-activated protein kinase kinase 1	305.5	18
3eocA	Cell division protein kinase 2	305.3	20
3eqgA	Dual specificity mitogen-activated protein kinase kinase 1	303.5	18
1finC	Cell division protein kinase 2	303.2	20
3eqbA	Dual specificity mitogen-activated protein kinase kinase 1	302.6	18
2jgzA	Cell division protein kinase 2	302.3	20
2h9vA	Rho-associated protein kinase 2	301.0	19

The score used to define similarity considers both sequence (profile-profile) and structural similarity. The ID column (percentage of sequence identity) refers to the structurally aligned residues.